

Mapping basin-wide subaquatic slope failure susceptibility as a tool to assess regional seismic and tsunami hazards

Michael Strasser · Michael Hilbe · Flavio S. Anselmetti

Received: 6 October 2009 / Accepted: 23 September 2010 / Published online: 22 October 2010
© Springer Science+Business Media B.V. 2010

Abstract This study of subaquatic slope failures in Lake Lucerne, central Switzerland, presents a new concept for evaluating basin-wide slope stability through time as a potential tool for regional seismic and tsunami hazard assessments. Previously acquired high-resolution bathymetry and reflection seismic data, as well as sedimentological and in situ geotechnical data, provide a comprehensive data base to use this lake as a “model basin” to investigate subaquatic landslides and related geohazards. Available data are implemented into a basin-wide slope model. In a Geographic Information System (GIS)-framework, a pseudo-static limit equilibrium infinite slope stability equation is solved for each model point representing reconstructed slope conditions at different times in the past, during which earthquake-triggered landslides occurred. Comparison of reconstructed critical stability conditions with the known distribution of landslide deposits reveals minimum and maximum threshold conditions for slopes that failed or remained stable, respectively. The resulting correlations reveal good agreements and suggest that the slope stability model generally succeeds

in reproducing past events. The basin-wide mapping of subaquatic slope failure susceptibility through time thus can also be considered as a promising paleoseismologic tool. Furthermore, it can be used to assess the present-day slope failure susceptibility, allowing for identification of location and estimation of size of future, potentially tsunamigenic subaquatic landslides.

Keywords Submarine landslides · Slope stability · Limit equilibrium · Paleoseismology · Lake Lucerne

Introduction

With increasing awareness of oceanic geohazards (e.g. Morgan et al. 2009), submarine landslides are gaining wide attention because of their potentially catastrophic impacts on both offshore infrastructures (e.g. pipelines, cables and platforms) and coastal areas (e.g. landslide-induced tsunamis; Locat and Lee 2002; Masson et al. 2006; Camerlenghi et al. 2007; and references therein). They also are of great interest because they may be directly related to primary trigger mechanisms including earthquakes, rapid sedimentation, gas release, glacial and tidal loading, wave action, or clathrate dissociation, many of which represent potential geohazards themselves (e.g. Hampton et al. 1996; Sultan et al. 2004; Owen et al. 2007; Lee et al. 2007; and references therein). In active tectonic environments, for instance, subaquatic landslide deposits can be used to evaluate the hazard derived from seismic activity (ten Brink et al. 2009a, b; Moernaut et al. 2007; Strasser et al. 2006; Goldfinger et al. 2003; Inouchi et al. 1996). Enormous scientific and economic efforts are thus being undertaken to better determine and quantify causes and effects of subaquatic landslides and related natural hazards.

Electronic supplementary material The online version of this article (doi:10.1007/s11001-010-9100-2) contains supplementary material, which is available to authorized users.

M. Strasser (✉)
MARUM, Centre for Marine and Environmental Sciences,
University of Bremen, Bremen, Germany
e-mail: mstrasser@marum.de

M. Strasser
Geological Institute, ETH Zürich, Zurich, Switzerland

M. Hilbe · F. S. Anselmetti
Eawag, Swiss Federal Institute of Aquatic Science
and Technology, Department of Surface Waters,
Dübendorf, Switzerland

In order to achieve this fundamental goal, the detailed study of past events, the assessment of their recurrence intervals and the quantitative reconstruction of magnitudes and intensities of both causal and subsequent processes and impacts are key requirements.

Instabilities of sediments along submerged slopes in both the marine and lacustrine environment occur where external driving forces that tend to deform and weaken sediments exceed the material strength properties that tend to resist such deformation (e.g. Sultan et al. 2004; Lee et al. 2007). Among the different possible driving forces of subaquatic slope instabilities, earthquake shaking is considered as an important trigger mechanism for tsunamigenic landslides (e.g. Hampton et al. 1996; Locat and Lee 2002; Owen et al. 2007; ten Brink et al. 2009b). Back-analyzing critical threshold conditions for past slope failure events that have been identified in the sedimentary record, and for which seismic shaking has been singled out as the external trigger mechanism, should thus allow for quantitative reconstruction of past earthquake intensities. Such quantitative paleoseismologic data may provide valuable information for understanding regional seismicity and for assessing the earthquake hazard.

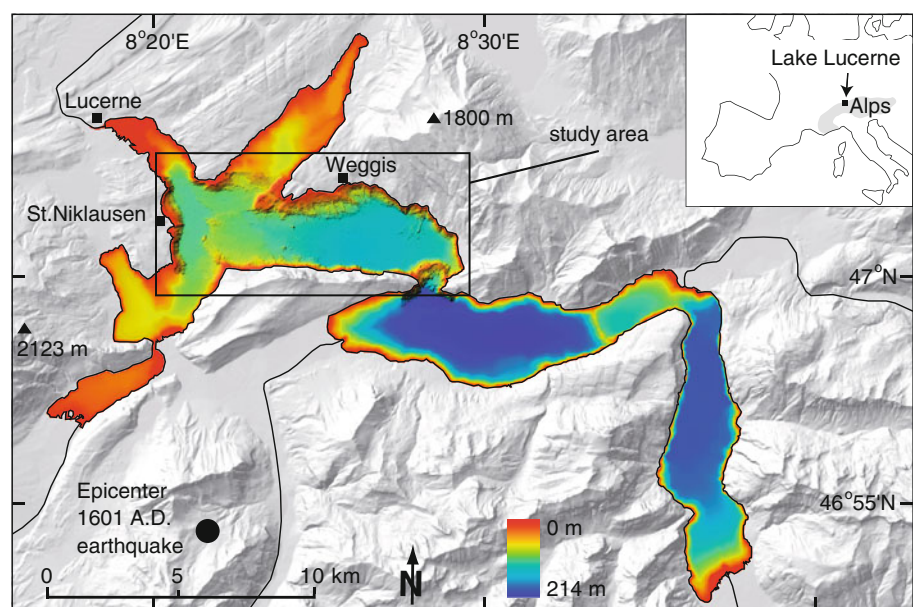
Here we present data and results from a study using Lake Lucerne in central Switzerland (Fig. 1) as a “model ocean” to test a new concept for the assessment of regional seismic and tsunami hazard by basin-wide mapping of critical slope stability conditions for subaquatic landslide initiation at different times in the past, during which earthquake-triggered subaquatic mass movements occurred. Because of their well-constrained boundary conditions, their smaller size and the possibility of being investigated on a complete basin-wide scale, studying slope failures in

lacustrine environments offers a series of advantages over marine examples (e.g. De Batist and Chapron 2008). State-of-the-art methods developed for oceanographic and geotechnical investigations can be utilized with fairly little logistical efforts and expenses to perform comprehensive studies. The resulting conceptual ideas can be vital to improve our understanding of larger marine slope failures and related seismic and oceanic geohazards (e.g. Kelts and Hsü 1980; Strasser et al. 2007; Girardclos et al. 2007; Moernaut et al. 2007).

In Lake Lucerne, previous studies have revealed the occurrence of earthquake-triggered tsunamigenic landslides during both historic and prehistoric times (Siegenthaler et al. 1987; Schnellmann et al. 2002, 2006) and provided first estimates on site-specific slope stability conditions during past seismic shaking events (Strasser et al. 2007). The well-constrained and comprehensive high-resolution bathymetry and reflection seismic data, as well as sedimentological and in situ geotechnical datasets from these studies provide an ideal basis for evaluating the potential of coupled temporal and spatial landslide inventories with basin-wide slope stability calculations through time, towards assessing regional seismic and tsunami hazard.

Previous applications of regional slope stability calculations using spatial data analysis in generic mapping tools or Geographic Information Systems (GIS) have successfully been implemented in many studies of landslide hazard assessment in both the subaerial (e.g. Mankelov and Murphy 1998; Miles and Keefer 2000; Gorsevski et al. 2006) and the submarine environment (e.g. Lee et al. 1999, 2000; Urgeles et al. 2002). What has been challenging so far, however, is to validate such regional slope stability models against actual occurrences of subaquatic landslides

Fig. 1 Overview map of Lake Lucerne and its surroundings (shaded relief topography from 25 m digital terrain model, Swisstopo) showing seven steep-sided subbasins with flat basin plains. The *rectangle* indicates the study area and outlines location of subsequent figures. *Black circle* in the SW corner of the map indicates estimated epicentral location of 1601 A.D. $M_w \sim 6.2$ earthquake (Schwarz-Zanetti et al. 2003; Gisler et al. 2004)



and—in the case of earthquake-triggered instabilities—use this approach as a quantitative paleoseismologic tool to reconstruct prehistoric ground-motion intensities independently from the earthquake focal mechanisms. Towards this goal, we (a) test the general Lake Lucerne sedimentological and geotechnical slope model by comparing spatially reconstructed critical slope stability conditions during past events with the known distribution of mass-movement deposits in the basin, (b) quantitatively reconstruct paleo-earthquake intensities needed to initiate the observed landslides, as well as (c) use the derived basin-wide model to identify slopes susceptible to future failure and (d) assess the related tsunamigenic potential.

Background and setting of Lake Lucerne

Lake Lucerne is a perialpine lake of glacial origin situated in central Switzerland and is characterized by several steep-sided subbasins with relatively flat basin plains (Fig. 1). Detailed descriptions of its glacial origin, morphology, general sedimentary infill, as well as postglacial evolution are given by Bühner and Ambühl (1996), Lemcke (1992), Schnellmann et al. (2005, 2006), Strasser et al. (2007) and references therein. This study concentrates on the lateral slopes of the external Chrüztrichter, Vitznau and Küssnacht Basins (Figs. 1, 2) that are separated from the major deltas by subaquatic sills.

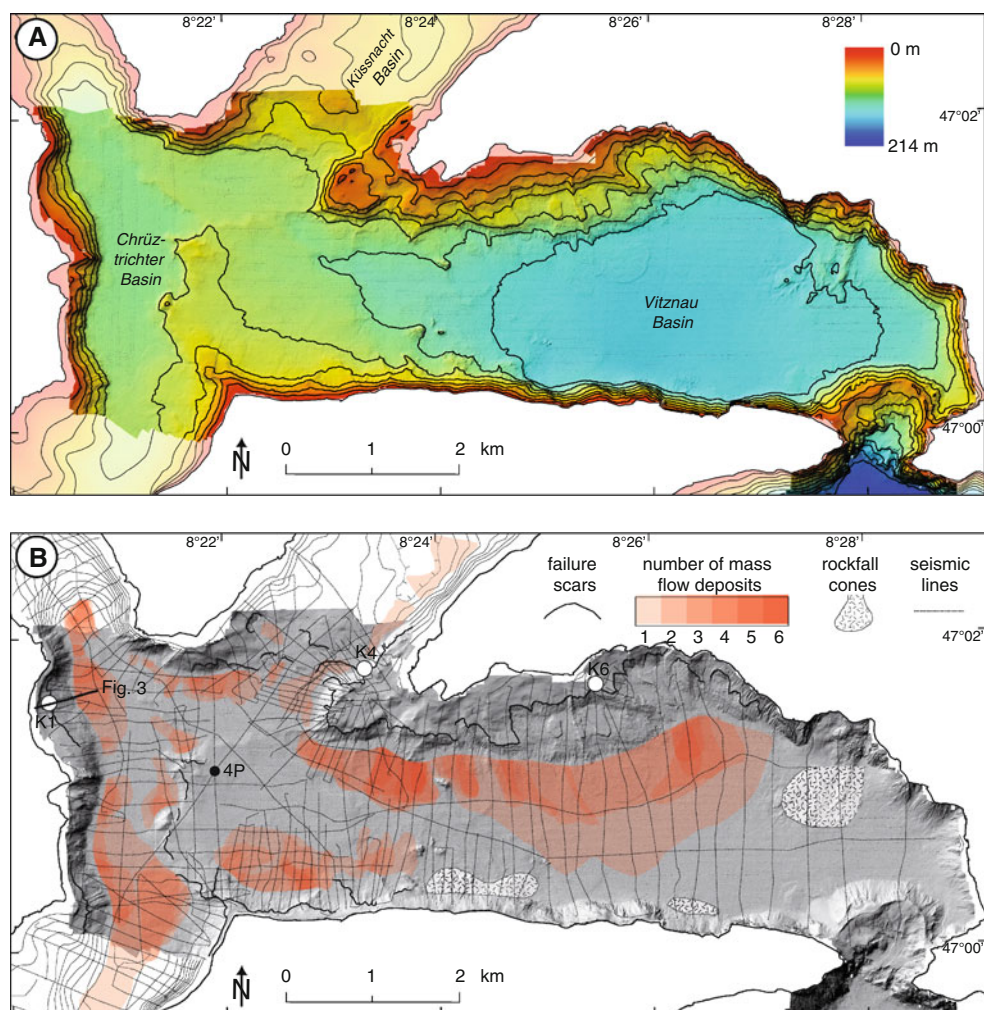


Fig. 2 **a** Bathymetry and shaded relief map of Chrüztrichter, Vitznau and Küssnacht basins from high-resolution swath bathymetry data (Hilbe et al. 2008; contour interval is 20 m; location in Fig. 1. **b** Shaded relief, available seismic lines and spatial distribution of subaquatic slide scars, mass-flow deposits and cones from subaerial rockfalls (Schnellmann et al. 2006). Intensities of red color indicate total number of stacked mass-flow deposits at the foot of slopes with

failures scars. **Bold line** indicates position of 3.5 kHz seismic profile presented in Fig. 3. **Open white circles** give positions of piston cores and in situ testing sites (4WS05-K1, K4 and K6; Strasser et al. 2007) and **black dot** indicates position of core 4WS00-4P (Schnellmann et al. 2006). Contour interval of area not covered by swath bathymetry is 10 m

In the postglacial sedimentary basin infill, several mass-movement units have been identified, six of which have been assigned to past earthquakes (i.e. multiple coeval slope failure events in 1601 A.D., around 2220, 9870, 11,600, 13,770 and 14,590 cal year. B.P.; Schnellmann et al. 2006). Seismically-triggered instabilities on the submerged lateral slopes generally occur as translational slides (Schnellmann et al. 2006; Strasser et al. 2007). Glide planes develop at the lithological boundary between overconsolidated glacio-lacustrine deposits with slightly elevated formation pore pressures below, and overlying slightly underconsolidated laminated Late Glacial clays characterized by low shear strength values at their base (Stegmann et al. 2007; Strasser et al. 2007). Previous studies identified the thickness of the postglacial sedimentary cover and thus the Holocene sedimentation rate, which shows significant spatial variations throughout the basin, to be a key parameter controlling the “charging” status of lateral slopes in Lake Lucerne (Schnellmann et al. 2006; Strasser et al. 2007).

The youngest of the units with coeval mass-movement deposits correlates to the historically described $M_w \sim 6.2$ earthquake in 1601 A.D. (Schwarz-Zanetti et al. 2003; Gisler et al. 2004) that triggered basin-wide subaquatic slope failures and subsequent tsunami and seiche waves as high as 3 m (Cysat 1601; Schnellmann et al. 2002, 2006). The temporal correlation of three prehistoric events recognized in Lake Lucerne with earthquakes reconstructed in Lake Zurich, situated ~ 40 km north of Lake Lucerne, suggests even stronger earthquakes ($M_w > 6.5$) at $\sim 2,220$, $\sim 11,600$ and $\sim 13,770$ cal. year B.P. (Strasser et al. 2006). However, there is only little quantitative information on effective ground-motion intensities in the Lake Lucerne area during these earthquakes. For the historic events, Monecke et al. (2004) estimated the macroseismic threshold intensity for basin-wide landsliding to be $I = VII$ (EMS 98) by calibrating the occurrence of multiple landslide deposits with macroseismic intensities reported in historical archives. Strasser et al. (2007) quantitatively investigated the slope stability conditions and slope failure initiation at three case study sites that failed during the historic 1601 A.D. and during the prehistoric Late Holocene earthquake around 2220 cal. year. B.P. Results provide first estimates on site-specific seismic threshold intensities for landslide initiation that are comparable with the historically reported macroseismic intensities for the 1601 A.D. event. While this match supports the adaptability of the reconstructed geological and geotechnical slope model and failure initiation mechanism at the three study sites, it remains to be tested whether these findings can be extrapolated on a basin-wide scale to regionally reconstruct intensities of past earthquakes and to eventually identify slopes susceptible to future tsunamigenic sliding.

Data and methods

Available datasets

The available well-constrained and comprehensive Lake Lucerne dataset comprises a complete temporal and spatial distribution of mass-movement deposits over the last 15,000 years, which is based on densely-spaced (~ 100 – 200 m), more than 300 km high-resolution 3.5 kHz seismic data, 10 long piston cores and 32 AMS- ^{14}C radiocarbon age dates (Fig. 2; Schnellmann et al. 2006). In addition, detailed sedimentological analysis and in situ geotechnical data provide quantitative information on strength characteristics along three submerged lateral slopes (Strasser et al. 2007). Furthermore, high-resolution bathymetric data with a grid spacing of 1 m and a vertical accuracy of a few decimeters acquired in 2007 using a swath bathymetry system (GeoAcoustics GeoSwath Plus, 125 kHz; Hilbe et al. 2008) allow for basin-wide bathymetric analysis and for detailed mapping of failure scars (Fig. 2).

Methods

In order to quantitatively assess basin-wide slope stability conditions during past (and potential future) landslide events, the geological and geotechnical slope model derived from the three case-study sites (Strasser et al. 2007) was extrapolated throughout the whole basin. Then, we deterministically solved a limit equilibrium infinite slope stability equation for individual model points representing reconstructed slope conditions at different points in time. This procedure reveals the spatial distribution of critical threshold values as a function of time. These results are then analyzed and compared with the known distribution of past mass-movement deposits using standard GIS-techniques.

In the following subsections the general concepts of slope stability calculations, model description, input parameters, model analysis, general assumptions and limitations are briefly outlined. A more detailed description of the general concepts in the electronic supplementary material (Online Resource ESM_1).

Infinite slope limit equilibrium analysis and its applicability to the Lake Lucerne study

The limit equilibrium infinite slope stability equation (Eq. 3 in Online Resource ESM_1; Morgenstern 1967; Seed 1979) evaluates the ratio between the downslope shear stresses acting on an inclined failure surface and the material-strength properties that tend to resist downslope movements. This ratio is known as the factor of safety (FS). Failure occurs when the effective mobilized shear

stress exceeds the maximum available shear strength ($FS \leq 1$). The material strength properties of water-saturated cohesive sediments (clayey silts and silty clays as recorded for Lake Lucerne lateral slope sediments; Strasser et al. 2007) are best described by the undrained shear strength (s_u ; Online Resource ESM_1).

For evaluating the stability of lateral, non-deltaic slopes in Lake Lucerne, the infinite slope assumption can safely be employed because (a) slope failures are characterized by translational sliding along well-defined planar sliding surfaces and (b) because the ratio between failure depth (in the order of 4–6 m for observed landslides) and the lateral extent of failure areas (ranging from a few 100 m to up to 3 km) is small enough that edge effects can be ignored.

In the stability calculation, the mobilized shear stress is the sum of the shear component of the gravitational load and additional seismic shear stresses approximated by including a pseudo-static acceleration (k) and assuming that the earthquake acceleration is applied over a significantly long period of time, so that the induced stress can be considered constant (Online Resource ESM_1; Seed and Idriss 1971). A limitation of this assumption is that the dynamic behavior of the sediment under cyclic loading conditions is not considered and additional effects, such as degradation of soft clays, accumulation of plastic strain and shear-induced excess pore pressure (Sultan et al. 2004; Biscontin et al. 2004) cannot be taken into account.

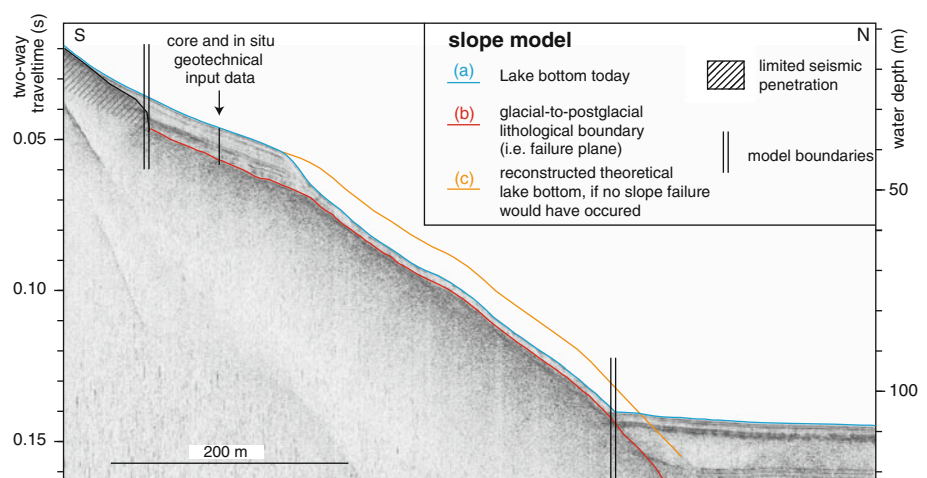
There are other factors in addition to gravity and seismic accelerations that need to be considered when evaluating driving-force components and effective stress conditions for subaquatic slope stability calculations, such as wave loading and excess pore water pressure (e.g. Lee and Edwards 1986; Dugan and Flemings 2000; Sultan et al. 2004). In Lake Lucerne, water depths in which slope failures occurs (>30 m) are sufficient to exclude strong waves (for this lake maximal 3–4 m high during extraordinary storms) as a source of downslope driving forces.

Concerning effective stress, results from the in situ geotechnical site characterization suggest that the pore pressures in the glacial deposits are slightly in excess of hydrostatic conditions (Stegmann et al. 2007; Strasser et al. 2007), thus lowering effective stress below the potential failure surface. Stegmann et al. (2007) conceptually interpreted that during past earthquake shaking, transient pore-pressure pulses migrated upwards from the overconsolidated section to the weak overlying postglacial section and played an important role in landslide initiation. The process and magnitude of overpressuring, however, remains uncertain. Because no quantitative information is available, it is beyond the scope of this study to account for the effect of transient excess pore pressures. For reasons of simplicity, the slope stability calculations in this study assume hydrostatic conditions at the failure surface and results thus may be afflicted with some uncertainties related to the effect of fluid overpressures, which was not considered here.

Input parameters for slope stability calculations

The slope stability equation (Eq. 3 in Online Resource ESM_1) for submerged slopes along a given potential failure surface in a function of the shear strength at the depth of failure, the severity of seismic shaking, the sediment density profile, the sediment thickness above the failure plane and the geometry of the slopes (i.e. slope angle). In Lake Lucerne, the stratigraphic position of the failure plane is well constrained, but its depth within the sedimentary profile increases with time due to continuous lacustrine sedimentation. Therefore, slope-stability conditions vary over time and also depend on the sedimentation rate along the submerged slopes. All of these controlling factors may vary regionally. Therefore, the geological and geotechnical slope model has to be constrained on a basin-wide scale prior to calculate slope-stability conditions.

Fig. 3 3.5 kHz seismic line illustrating the typical slope geometry and sedimentary cover of lateral non-deltaic slopes in Lake Lucerne that failed during past earthquakes (example: St. Niklausen Slide of Schnellmann et al. 2005; location in Fig. 1). Superimposed interpretation as implemented into the slope model and location of site 4WS05K1, where sedimentological and geotechnical data have previously been acquired (Strasser et al. 2007)



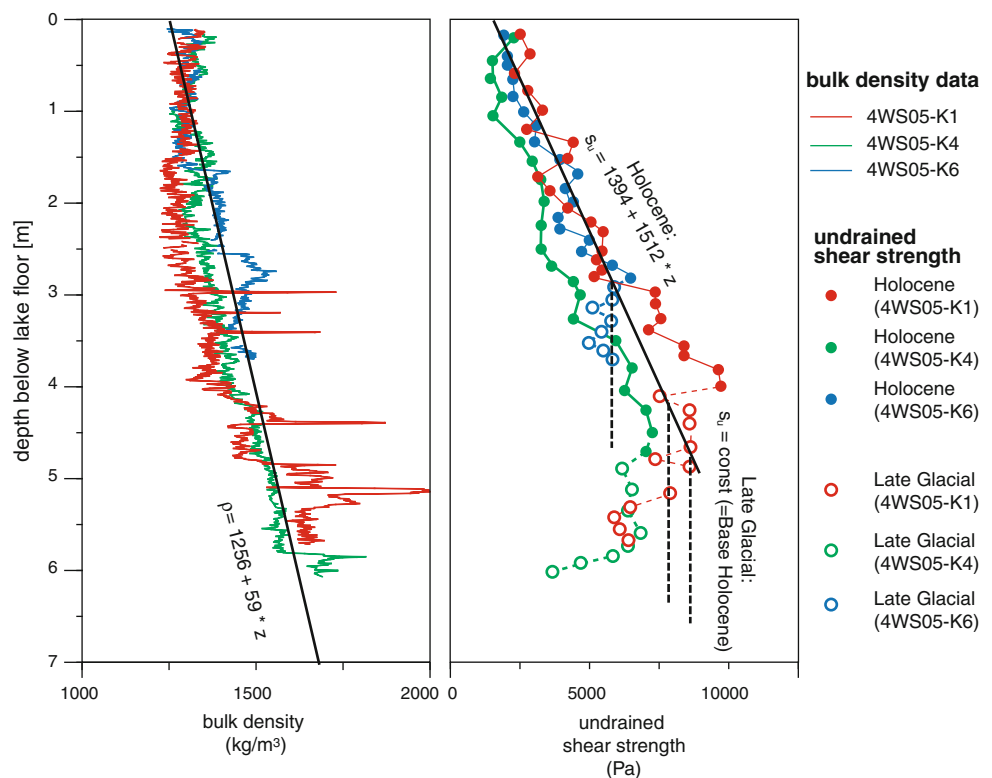
Slope geometry In the seismic data the lake floor reflection (horizon a; Fig. 3) and the reflection corresponding to the glacial-to-postglacial lithological boundary (horizon b; i.e. failure surface; Strasser et al. 2007) were systematically mapped over the whole study area using the seismic interpretation software Kingdom Suite. Additionally, a third horizon (c) reconstructs the theoretical water bottom approximating the slope geometry for the present-day situation if no landslides had occurred in the past (Fig. 3). The reconstruction assumes constant sediment thickness draping the slopes along individual seismic lines. This assumption is justified by bathymetry and seismic data that show smooth surface textures and constant sediment thicknesses, respectively, in undisturbed sections adjacent to failed slopes. Furthermore, it is assumed that the sediment cover adjacent to failure scars represents the continuous undisturbed postglacial sedimentary section, as recovered in cores from the three case study sites (Strasser et al. 2007).

Along each seismic line, single data points (point spacing 10 m) containing depth information of all three mapped horizons were exported from the seismic interpretation software and transferred into a GIS environment (ArcGis 9.2). The model boundaries for each single line were defined at the sharp slope break between the lateral slope and the basin floor and in shallow areas, where seismic penetration is limited (Fig. 3). Two-way travel time was converted to water depth and sediment thickness using a constant velocity of $1,450 \text{ ms}^{-1}$ (Strasser et al. 2007), and absolute offsets

were corrected to fit with the actual measured water depth. In the GIS software the geological model as mapped in the seismic data is represented by a point-source data set with high data density along seismic lines and no information between them. It was tested in a first attempt to interpolate the point-source data to raster data (e.g. testing spatial interpolation of seismic horizon a (i.e. lake floor picked from seismic data) against multibeam lakefloor bathymetry), with the aim of performing a grid-based slope stability analysis over the whole study area. Line spacing of seismic data, however, does not allow for meaningful interpolation of high-resolution grids (i.e. $>10\%$ deviation between interpolated water depths from seismic data and depth values from multibeam bathymetry for areas between seismic lines). Such systematic errors induced by gridding algorithms and their propagation during subsequent analysis, in particular for horizons b and c, significantly tamper results of the slope stability analysis. Therefore, all analyses were performed within the point-source data set to reduce uncertainties and error propagation to a minimum. Only slope angles were calculated on the basis of the bathymetry dataset resampled to a grid spacing of 10 m.

Geotechnical properties Bulk density (ρ) and undrained shear strength (s_u) values for model input data are derived from the results of the detailed sedimentological and in situ geotechnical site characterizations at three case study sites (Strasser et al. 2007; see Fig. 2 for locations of sites).

Fig. 4 Bulk density (ρ) and undrained shear strength (s_u) measured at three case study sites (Strasser et al. 2007). *Black and dashed lines* show density and Holocene strength gradients, and constant Late Glacial strength conditions, respectively, used as input for the slope stability assessment. Core locations in Fig. 2



All three sites reveal comparable stratigraphic, sedimentological and physical-property characteristics of the post-glacial drape overlying the potential failure plane at the glacial-to-postglacial lithological boundary. In general, ρ continuously increases with depth at all three sites (Fig. 4a). Hence, density profiles can be approximated in the basin-wide model with a linear function:

$$\rho(z) = \rho(0) + \nabla\rho \cdot z \tag{1}$$

with $\rho(0)$ corresponding to the bulk density at the top of the sedimentary profile and $\nabla\rho$ representing the gradient of density increase with depth. Best-fit mean values are $\rho(0) = 1,256 \text{ kg/m}^3$ and $\nabla\rho = 59 \text{ kg/m}^3/\text{m}$ (correlation coefficient $R^2 = 0.85$).

Undrained shear-strength values (s_u) also generally increase with depth in the Holocene section and suggest normal consolidation for the Holocene deposits (Fig. 4b). The Late Glacial sedimentary section, however, shows generally constant or even slightly decreasing s_u values and suggests underconsolidation in the lower part of sedimentary section. Strasser et al. (2007) interpreted this observation to be related to unfavorable strength characteristics of faintly laminated Late Glacial clay deposits immediately overlying the potential failure plane. In order to account for the different strength distribution in the Holocene and Late Glacial section, s_u values are approximated using a two-layer model with

$$s_u(z) = s_u(0) + \nabla s_u \cdot z \tag{2}$$

for the Holocene section, with $s_u(0)$ corresponding to the undrained shear strength at the top of the sedimentary profile and ∇s_u representing the gradient of strength increase with depth. Best fit mean values are $s_u(0) = 1,394 \text{ Pa}$ and $\nabla s_u = 1,512 \text{ Pa/m}$ (correlation coefficient $R^2 = 0.89$); and

$$s_u(z) = \text{const} = s_u(z = d_H) \tag{3}$$

for the Late Glacial section, with d_H being the thickness of Holocene drape. Although correlation coefficients for the linear interpolation of ρ and s_u (Holocene) are relatively high and thus legitimize the assumption of one single physical-property model as input for the regional slope stability analysis, it has the shortcoming that possible small regional variations in these parameters cannot be considered.

Sedimentation rate and sediment thickness While the reconstructed sedimentation rates on the lateral slopes during Late Glacial times at all three case study sites are

constant in the order of 22 cm/ky ($\pm 0.2 \text{ cm/ky}$), they vary significantly from site to site (22–42 cm/ky) during Holocene times (Strasser et al. 2007). This suggests large variations in sediment thickness above the potential failure surface across the study area, as also indicated in the seismic data. To account for this regional thickness variation, as well as for changes in thickness as a function of time, variable Holocene sedimentation rates are used as input parameters for the stability calculations. The Late Glacial sedimentation rate is kept constant at 22 cm/ky. Holocene sedimentation rates are assessed for each individual data point by calculating the theoretical thickness (i.e. depth of horizon b minus depth of horizon c; Fig. 3), from which the thickness of the Late Glacial section is subtracted (i.e. Late Glacial sedimentation rate multiplied by the Late Glacial duration, assumed to be $\sim 6,000$ years, from $\sim 17,500$ to 11,500 cal year B.P.; see Strasser et al. 2007 for details) and dividing the resulting Holocene thickness by the duration of the Holocene ($\sim 11,500$ years).

Basin-wide slope stability analysis: methodological approach

All input parameters mentioned above (summarized in Table 1) were assigned to each single data point in the GIS point-source data set, for which the limit equilibrium infinite slope stability can then be evaluated. The calculations were performed in a deterministic approach that uses one single value for each input parameter. Therefore, uncertainties and natural variations of model input parameters were not taken into account. Two different types of slope stability analysis were carried out. They are briefly outlined in the following sections.

Back-analysis of past slope failure events The back-analysis approach assumes $FS = 1$ at failure and tries to constrain the critical parameter that could produce instability. Because past subaquatic landslides in Lake Lucerne are mainly triggered by earthquake shaking, the critical parameter of interest in this study is the pseudo-static acceleration (k). Substituting s_u , σ' and σ in the general slope stability equation (Eq. 3 in Online Resource ESM_1) with the physical-property models (Eqs. 1, 2 and 3), assuming hydrostatic conditions and solving the equation for critical k (k_{crit}) then reveals:

$$k_{crit} = \frac{s_u(0) + \nabla s_u \cdot (z - d_{LG}) - 1/2 \cdot (2 \cdot \rho(0) - 2 \cdot \rho_w + \nabla\rho \cdot z) \cdot g \cdot z \cdot \sin \alpha \cdot \cos \alpha}{1/2 \cdot (2 \cdot \rho(0) + \nabla\rho \cdot z) \cdot g \cdot z \cdot \cos^2 \alpha} \tag{4}$$

Table 1 Parameters used for slope stability calculations

Input parameter	Value	Data derived from
Undrained shear strength at the top of the sedimentary profile, $s_u(0)$ (Pa)	1,394	Case studies by Strasser et al. (2007); see Fig. 4
Gradient of strength increase with depth, ∇s_u (Pa/m)	1,512	Case studies by Strasser et al. (2007); see Fig. 4
Bulk density at the top of the sedimentary profile, $\rho(0)$ (kg/m ³)	1,256	Case studies by Strasser et al. (2007); see Fig. 4
Gradient of bulk density increase with depth, $\nabla \rho$ (kg/m ³ /m)	59	Case studies by Strasser et al. (2007); see Fig. 4
Slope angle, α (°)	Varying for each data point	Swath bathymetry data by Hilbe et al. (2008)
Sediment thickness above failure plane, z (m)	Varying for each data point	Seismic data by Schnellmann et al. (2006); see Fig. 3
Late Glacial sedimentation rate (cm/ky)	0.22	Case studies by Strasser et al. (2007)
Holocene sedimentation rate and sediment thickness	Varying for each data point	SEISMIC data by Schnellmann et al. (2006)
Gravitational acceleration, g (m/s ²)	9.81	

Limit equilibrium infinite slope stability model (Morgenstern 1967), undrained failure under hydrostatic conditions along the glacial-to-postglacial lithological boundary, pseudo-static horizontal accelerations represent seismic ground accelerations (i.e. model does not consider dynamic effects during seismic shaking), constant sediment thickness perpendicular to slopes, no slope failure occurred prior to the reconstructed moment in time

with ρ_w = water density (1,000 kg/m³), z = depth of failure and d_{LG} = thickness of the Late Glacial section.

Equation 4 can be solved for each single data point in the GIS point-source data set for specific past moments in time by calculating the corresponding depth of failure for each point at each time step using the reconstructed Holocene sedimentation rates. The resulting regional distribution of k_{crit} values then can be compared with the corresponding distribution of mass-movement deposits and landslide scars (Schnellmann et al. 2006). This comparison was carried out with a statistical approach: slope areas that failed or remained stable during each individual event were first mapped and then spatially analyzed for minimum, maximum and mean k_{crit} values using the “zonal statistics tool” implemented in the GIS software package ArcGIS 9.2. Note that the input slope model for the back-analysis assumes that no slope failures occurred prior to analysis at each individual point. This limitation locally may not represent the actual slope history, because some stacked mass-flow deposits in the basin suggest that some slopes repeatedly failed and/or retrogressive failure occurred (Schnellmann et al. 2006).

Forward-modeling and slope failure susceptibility assessment With the aim of identifying slopes susceptible for failure today (or in the future), and in order to eventually assess the landslide and tsunami hazard in Lake Lucerne, deterministic limit-equilibrium calculations simulating different earthquake scenarios (i.e. varying input values for k) also can be applied to the slope model for the present-day or future situations. To account for the fact that slopes that already failed in the past show different strength characteristics, because the underconsolidated Late Glacial clays

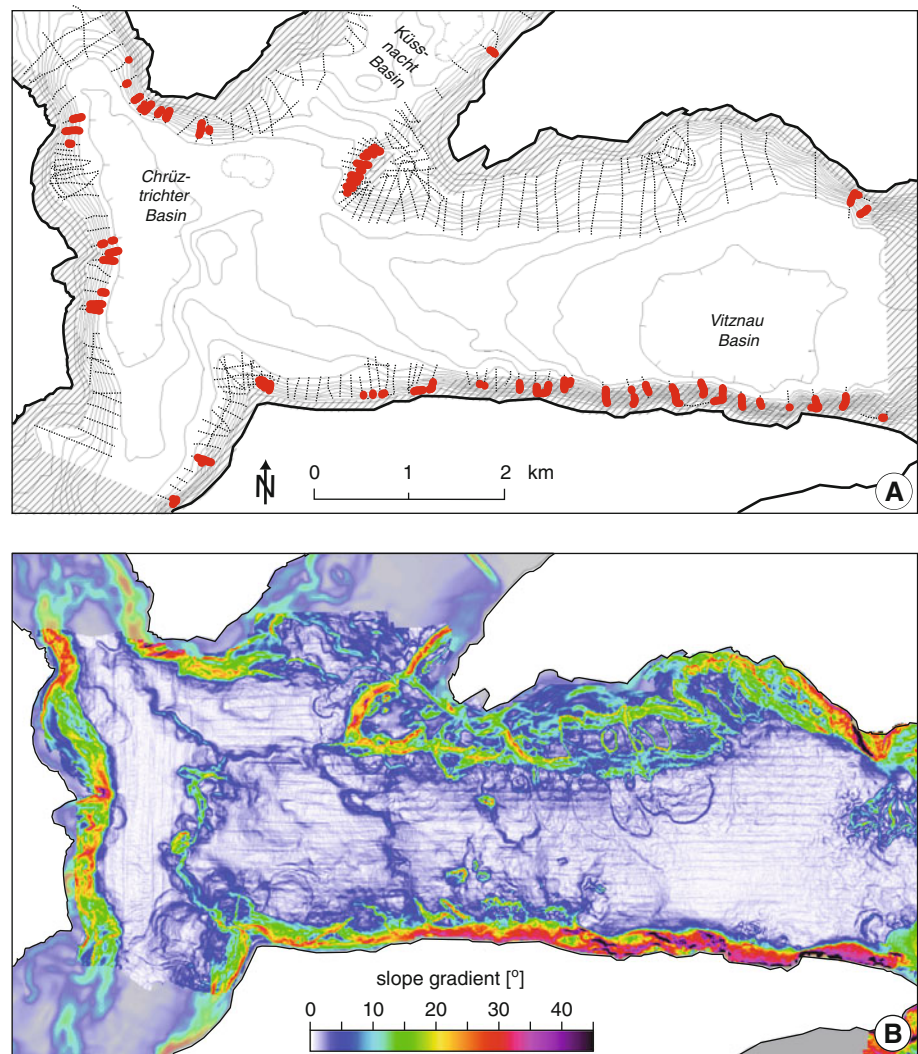
have already slid away, the model for the geotechnical input parameters needs to be revised. Therefore, it is assumed that along previously eroded slopes the potential failure plane is only covered with Holocene sediments, the physical properties of which can be approximated by Eqs. 1 and 2. Slopes that have remained stable throughout the past are modeled as outlined above for the back-analysis approach.

Sensitivity analysis and limitation

In order to gain better understanding how the model input parameters interact and how they influence the resulting slope stability calculations, a sensitivity analysis was carried out (Online Resource ESM_2). Results imply that the defined slope model does not reproduce slope stability conditions older than ~11,500 years ago and the oldest possible model boundary thus has to be defined to that age. Therefore, back-analyses are carried out for Holocene events only. The most sensitive input parameters are the physical property parameters ($s_u(0)$, ∇s_u and $\rho(0)$). The resulting critical acceleration may vary in the range of ± 1 –2% g , when considering uncertainties of absolute values in these three input variables.

Additionally, the sensitivity analyses and critical seismic-acceleration calculations for representative data points situated along the bathymetric sill separating the Chrüztrichter and Vitznau Basins (see Fig. 2 for location) reveal odd results suggesting that the chosen sedimentological and physical properties do not properly represent the true conditions in this area. We suggest that postglacial sedimentation patterns in this area, especially during Late Glacial times, were significantly different than along the

Fig. 5 a Combined results of slope stability assessments for static loading conditions simulating different time steps during the last 11,500 years. *Red dots* indicate slope segments that were statically unstable ($FS \leq 1$) throughout the past and therefore lack a considerable sediment cover. *Fine black dots* indicate areas that are stable under static loading conditions and thus are interpreted to only become unstable if additional external trigger mechanisms (i.e. seismic shaking) drive the slope toward failure. *Hatched areas* indicate model boundaries. **b** Slope angles calculated from high-resolution bathymetry data resampled to 10 m cell size or interpolated from seismic data for area outside the bathymetry data coverage



lateral slopes, where input data for the slope model were defined, as indicated by comparison between core 4WS00-4P (Schnellmann et al. 2006; see Fig. 2 for location) and cores from the three case study sites (Strasser et al. 2007). Therefore, this area was not included in the basin-wide slope stability assessment.

Results from basin-wide slope stability calculations

Slope stability under static loading conditions

A first basin-wide analysis was performed in order to investigate slope stability under static loading conditions. For each single data point in the GIS point-source data set, factors of safety (FS) were calculated for the present-day slope and for the reconstructed slope conditions at selected times over the last 11,500 years, during which subaquatic landslide events occurred. Figure 5 shows all data points that revealed statically unstable stability conditions

throughout the last 11,500 years (i.e. $FS \leq 1$). The spatial distribution of the identified statically unstable areas corresponds to steep slopes (inclination angles $>22^\circ$; Fig. 5b) that lack a major sedimentary cover and that are often characterized by slightly wedge-shaped lower slope-break geometries towards the basin plain, as indicated in seismic and bathymetric data. This observation clearly suggests that such slope areas are too steep to allow permanent accumulation of sediments and that sediment remobilization and/or creeping processes are continuously acting on these slopes. Slopes with inclination angles $<20^\circ$ are statically stable with $FS > 1.1$ and thus are interpreted to become unstable only if additional external trigger mechanisms (i.e. seismic shaking) drive the slopes toward failure.

Pseudo-static slope stability back-analysis

Maps presented in Fig. 6 show calculated critical pseudo-static horizontal accelerations (k_{crit}) required for slope instability at each data point in the GIS point-source data

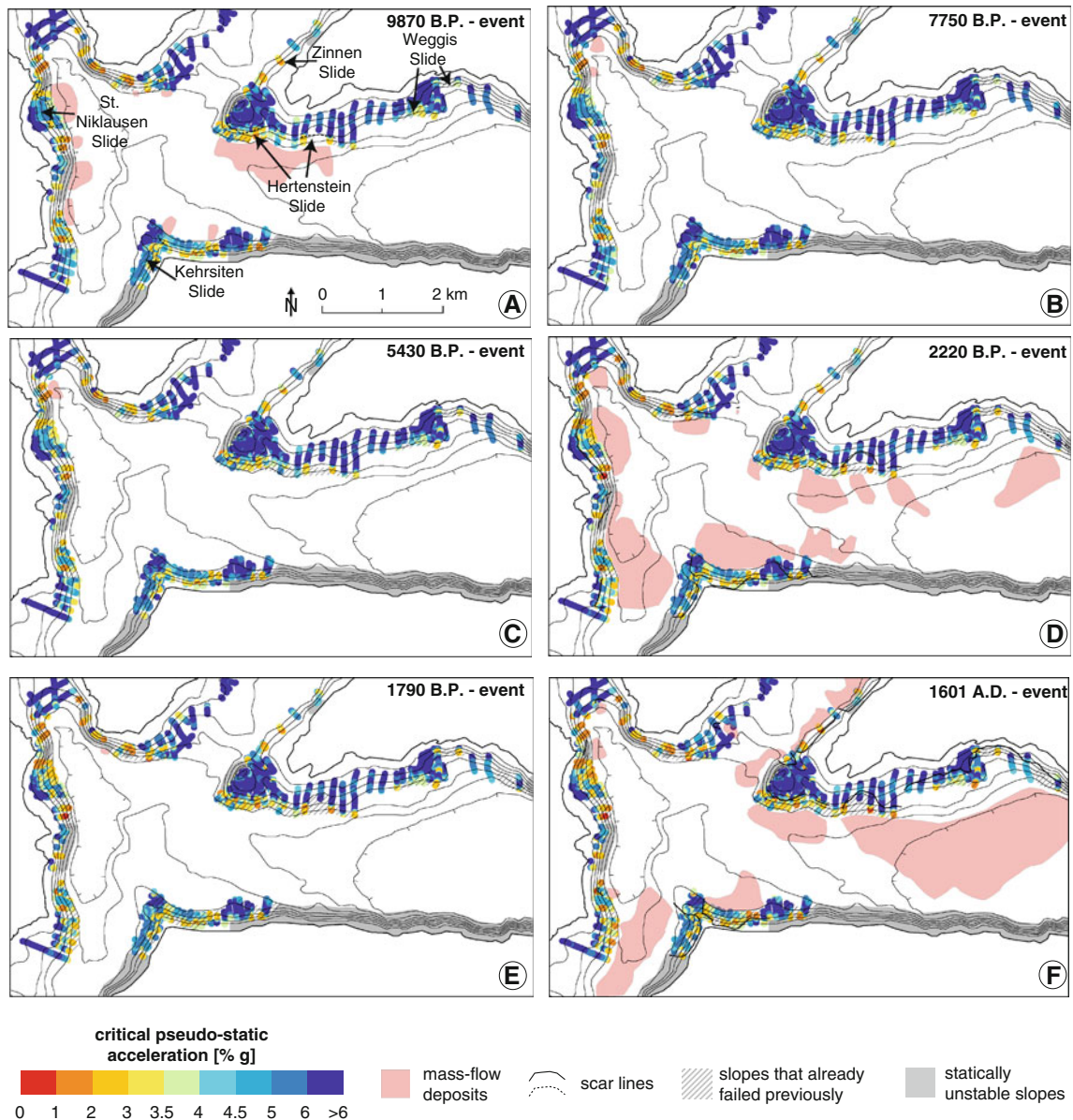


Fig. 6 Results of slope stability calculations showing critical pseudo-static horizontal accelerations (k_{crit}) required for slope instability reconstructed for past moments in time, during which subaquatic landslide events occurred. Note that stability assessments in areas

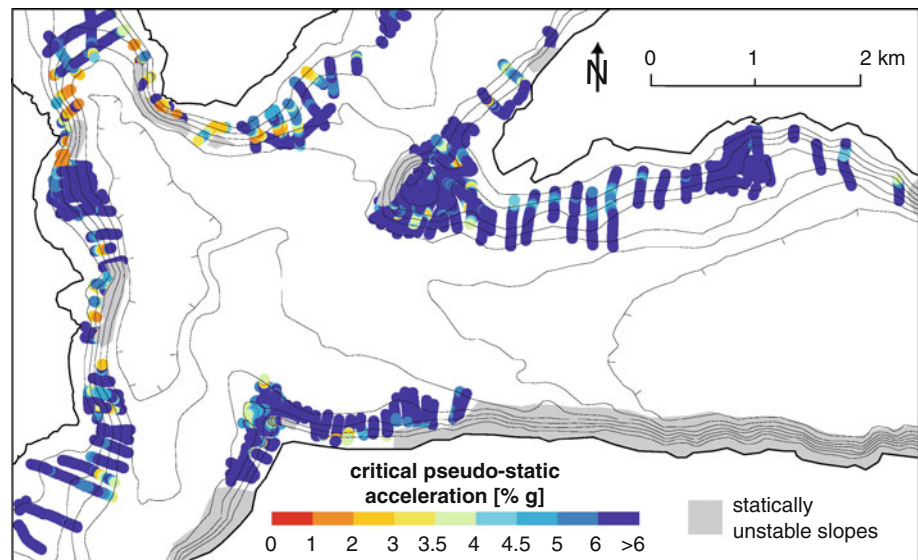
that already failed previously (*hatched areas*) may reveal too low k_{crit} values, because effective thickness may be reduced if part of the section already slid away previously. **a** Locations of specific areas discussed in the text

set representing reconstructed pre-landslide slope conditions at specific times in the past, during which subaquatic landslide events occurred. Low threshold values (i.e. green, yellow and orange colors in Fig. 6) are generally found in interpreted source areas of larger mass flows, the deposits of which have been identified in the basin plain sediments close the slope breaks (mapped as red-colored areas in Fig. 6; Schnellmann et al. 2006). High critical threshold values (i.e. blue colors in Fig. 6) occur upslope of mapped landslide scars and along slope segments that are characterized by undisturbed, continuous slope covers and adjacent basin plain sedimentary successions that lack evidence

of mass-flow deposits. This correlation of low and high critical pseudo-static accelerations with areas that failed and remained stable, respectively, during all investigated past events suggests that the slope stability model generally succeeds in reproducing past subaquatic mass-movement events.

Results reveal k_{crit} values up to $\sim 4\%$ g for reconstructed limit equilibrium slope stability conditions of areas that failed during past events. Overall, slope stability slightly decreases from older toward younger ages (i.e. decreasing k_{crit} values in the order of $\sim 1\%$ g over the last 10,000 years) reflecting increased sediment “charging”

Fig. 7 Present-day slope stability situation showing critical pseudo-static horizontal accelerations to cause subaquatic landslides in Lake Lucerne. Low values (*reddish colors*) indicate high slope failure susceptibility



through time. This is, for instance, illustrated in Fig. 6 for the source area of the St. Niklausen Slide complex (see Fig. 6a for location) by changing from bluish-green colors at 9870 year. B.P. to orange colors by 1601 A.D. In areas where slope failures already occurred prior to the analyzed moment in time (hatched areas in Fig. 6), however, the result might be biased because the model assumes that the reconstructed pre-landslide slopes represent undisturbed conditions of the entire continuous postglacial sedimentary strata. We do not consider whether older landslides in such areas eroded the entire slope up to present-day failure scar positions (Fig. 2) or if older instabilities only occurred in lower slope regions and younger events retrogressively mobilized sediments towards mid- to upper slope regions. The latter scenario is likely to have occurred in areas where model calculations generally reveal lower stability conditions in lower slope areas (e.g., St. Niklausen, Hertenstein and Weggis Slide complexes; see Fig. 6a for location).

In the northern part of the study area, along the NW-dipping slope of the Küssnacht Basin (source area of Zinnen Slide; see Fig. 6a for location), critical threshold accelerations are relatively low throughout Holocene times, but seismic data only indicate mass-movement deposits related to the youngest 1601 A.D. earthquake event (Schnellmann et al. 2005). Therefore, the slope stability model may not fully reproduce the proper stability conditions in this area, presumably due to the fact that data coverage in this area is insufficient. In contrast, slope stability along the lower slope region in the source area of the Kehrsiten Slide complex (see Fig. 6a for localization) appears to be rather high for a slope that failed during the 2220 years B.P and 1601 A.D. events. However, the upper slope of this area shows relatively low k_{crit} values, suggesting that the lowest threshold value over the whole failure area controls failure initiation.

Present-day slope stability assessment

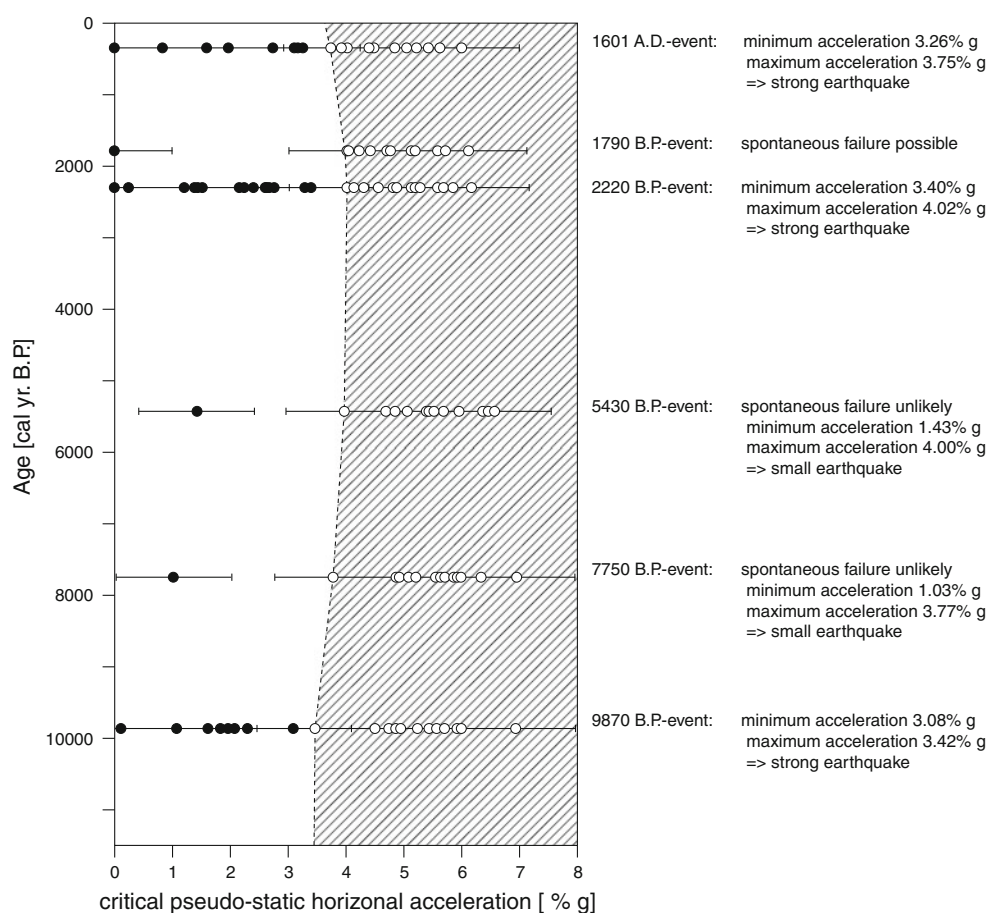
In order to assess present-day slope failure susceptibility along subaquatic slopes of the studied subbasins in Lake Lucerne, critical pseudo-static accelerations (k_{crit}) were calculated for the present-day situation (Fig. 7). Results suggest that most slope areas, apart from the steep slopes that are unstable under static loading conditions, today are relatively stable. However, in the northwestern part of the study areas, towards the Bay of Lucerne, calculated k_{crit} values required to initiate landslides are locally relatively low, suggesting high slope failure susceptibility. Such areas generally correspond to slope segments that are characterized by relatively high sedimentation rates and that have repeatedly been active in the past, and thus can be considered as “hot spots” for subaquatic landslides in Lake Lucerne. Landslides in these critical areas, however, are generally relatively small compared to their larger counterparts (e.g. St.Niklausen, Kehrsiten, Hertenstein and Weggis Slide complexes), as higher recurrence rates prevent the slopes from being covered with thick sedimentary successions. In the western part of the study area, especially along the submerged slopes offshore Weggis, only few data points reveal critical accelerations close to values that have been reached during past earthquake events.

Interpretation and discussion

Paleoseismologic reconstructions

In order to quantitatively back-analyze individual past earthquake-triggered landslides and, eventually, to reconstruct seismic intensities in the Lucerne area, the

Fig. 8 Compiled results from slope stability back-analysis showing minimum critical pseudo-static accelerations for individual slope areas, at the bottom of which landslide deposits occur for the corresponding times (*black dots*), or which show undisturbed postglacial sedimentary successions in the seismic data indicating stable conditions throughout the past (*open circles*). *Hatched area* thus indicates paleo-earthquake intensities that were never exceeded during the past 11,500 years. Right-hand side: quantitative paleoseismologic interpretation for individual events (see text for detailed discussion)



distribution of k_{crit} along individual slope areas for the different moments in time, as presented in Fig. 6, was statistically analyzed. The failure criterion was defined as representing the lowest k_{crit} value for each individual slope area. This assumption provides conservative estimates on minimum earthquake intensities that were reached and maximum values that were not exceeded, as revealed by zonal statistical analyses along slopes that failed or remained stable, respectively. Figure 8 presents the compiled results of all zonal statistical analyses. Black dots show minimum k_{crit} values for each mapped slope segment, at the bottom of which landslide deposits occur for the corresponding times. White dots give minimum k_{crit} values needed to initiate failure along slopes that remained stable throughout the past, as indicated by smooth lake floor and undisturbed postglacial sedimentary successions in the bathymetry and seismic data, respectively. For each individual event, the highest plotted k_{crit} value reconstructed for failed slope segments indicates the minimal acceleration that was reached in the study areas, whereas the lowest value reconstructed for slopes that remained stable indicates maximal acceleration that was not exceeded.

Reconstructed minimum and maximum threshold conditions do not overlap for any investigated past event and

thus suggest that the used sedimentological, geotechnical and stability models generally succeed in reproducing basin-wide slope conditions along lateral non-deltaic slopes in the study area over the last 11,500 years. Results confirm the interpretation by Schnellmann et al. (2006) that the three major slope failure events showing coeval landslide deposits throughout the basin can be related to strong seismic shaking in the study area corresponding to k_{crit} values between 3.26–3.75, 3.4–4.02, and 3.08–3.42% g for the 1601 A.D., 2220 years B.P., and 9870 years B.P. events, respectively. The three smaller events characterized by only one or two landslide deposits can either have been initiated spontaneously (1790 years B.P. event) or may be related to minor local ground shaking during small earthquakes events around 5430 and 7750 cal years. B.P. corresponding to k_{crit} -values of 1.43 and 1.03% g, respectively. While positive evidence of reached seismic accelerations is limited to the observed six events, we can exclude the possibility that maximum values of k_{crit} ever exceeded values that plot in the hatched area shown in Fig. 8, because otherwise we would observe mass-flow deposits in the basin related to such an event.

The pseudo-static horizontal acceleration, as used in this study to model the additional earthquake-induced shear

stress driving subaquatic slopes towards failure, cannot be directly compared to the seismic peak ground acceleration (PGA), the parameter generally used for seismic hazard assessments. PGA values are usually higher (Seed and Idriss 1971; Seed 1979) and pseudo-static horizontal accelerations as the average equivalent uniform shear stress imposed by seismic shaking only represent $\sim 65\%$ of the effective seismic peak ground acceleration (Seed and Idriss 1971). Having taken this into account, results from the slope stability back-analysis suggest that past earthquakes in the Lucerne area may have reached PGAs as high as $\sim 5.2\text{--}6.2\%$ g during the presumably strongest event of the last 11,500 years that occurred around 2220 cal. years B.P. On the other hand, the data suggest that PGA never exceeded maximal values of $\sim 6.2\%$ g during the investigated time period. The reconstruction of the historically documented 1601 A.D. event (i.e. $\sim 5.0\text{--}5.8\%$ g peak ground acceleration) lies in the range of calculated values deduced from predictive ground-motion models (Bay et al. 2005) and suggests comparable macroseismic threshold intensities (PGA-to-intensity correlation function by Murphy and O'Brien 1977), as estimated from historic data ($I = \text{VII}$; Schwarz-Zanetti et al. 2003). These findings thus indicate that the proposed slope stability modeling approach reveals robust results and can be considered and as a promising tool for reconstructing past slope stability conditions, providing quantitative information on intensities of past seismicity in the Lucerne area.

Identifying slopes susceptible for future earthquake-triggered tsunamigenic sliding

It has been shown in previous studies that subaquatic landslides in Lake Lucerne can trigger tsunami and seiche waves (Siegenthaler et al. 1987; Schnellmann et al. 2002, 2006). Among several parameters that control the tsunamigenic potential of subaquatic landslides, the slide volume, which defines how much water is displaced as a consequence of the downslope moving landslide mass, is an important parameter (e.g. Trifunac and Todorovska 2002; Bardet et al. 2003). The slide volume directly depends on the thickness of the slope segment that is mobilized during landsliding. The basin-wide slope model of Lake Lucerne allows us to calculate the thickness of potentially unstable slope segments and thus may provide initial “proxy” data toward assessing the tsunamigenic potential of slopes susceptible for future landsliding. To achieve this goal, different scenarios of earthquakes that may hit the study area in the future were evaluated. Forward-modeling the limit equilibrium slope stability condition for each data point in the GIS point-source data set using different pseudo-static accelerations (i.e. simulating different earthquake scenarios) reveals the basin-wide

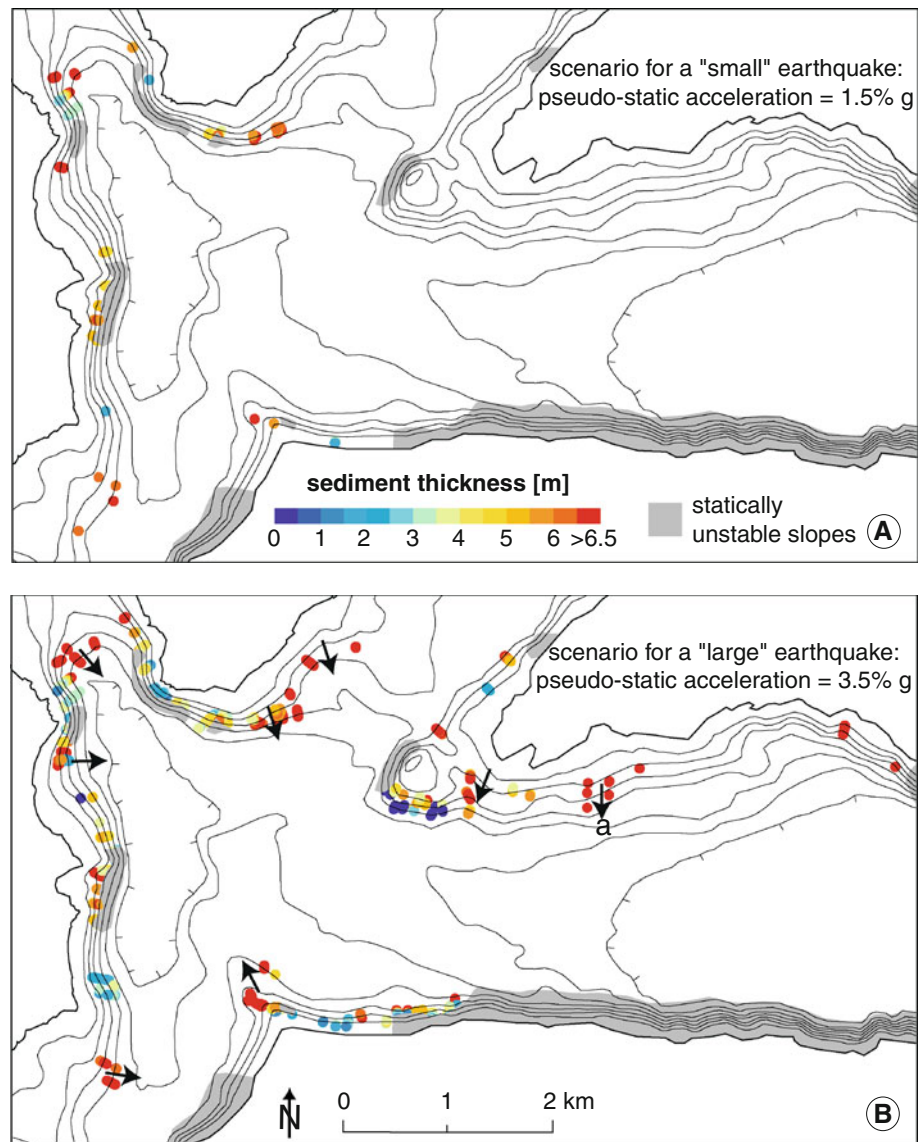
distribution of FS under the modeled earthquake conditions for the present-day situation. In the resulting maps, data points with $FS < 1.1$ can be plotted as a function of their sediment thickness, which would be mobilized if slope failures occur (Fig. 9). Note that $FS = 1.1$ was chosen as the failure criterion in order to conservatively account for uncertainties in the slope stability model. A first-order estimate on tsunamigenic landslide susceptibility in the study area then corresponds to the sediment thickness along potentially unstable slopes.

Results reveal that seismic ground shaking corresponding to pseudo-static horizontal accelerations of 1.5% g (simulating small earthquake intensities with PGAs of $\sim 2.5\%$ g) may locally initiate failure along slopes of the Chrüztrichter Basin that are covered with >5 m of postglacial sediments (Fig. 9a), providing the potential for triggering small tsunami waves. If a larger earthquake, comparable to the 1601 A.D. or even the 2220 years B.P. event, would hit the Lucerne area again (assumed $k = 3.5\%$ g; i.e. mean value between reconstructed minimum and maximum accelerations for the 1601 A.D. event) slope failures might occur throughout the basin (Fig. 9b). Especially in slope regions that remained stable during the 1601 A.D. event, and thus may still be sufficiently “charged”, as well as larger slope areas covered with >5 m sediment that would be mobilized during such a potential future event (areas marked with arrows in Fig. 9b). A slope segment offshore Weggis (labeled “a” in Fig. 9b, for instance, then may reach comparable dimensions to the 2220 years B.P. Kehrsiten Slide, that was modeled by Schnellmann et al. (2002) to have triggered tsunami waves with amplitudes up to 3 m.

General considerations and outlook

Although our slope stability analysis generally reveals robust results that are in agreement with the observed distributions of past landslide and historic paleoseismologic reconstruction, absolute values derived from the deterministic limit-equilibrium calculations may only be considered as first-order estimates, because the model has several shortcomings that need to be addressed before being eventually implemented into realistic seismic and tsunami hazard assessments for the Lake Lucerne area: The current basin-wide slope model assumes one single physical property model to be representative for all lateral slopes in the study area. This has the shortcoming that small regional variations in strength parameters cannot be considered. To account for regional variations in physical property conditions in the basin-wide stability analysis, however, data from more than just three sites is needed. A time- and cost-efficient approach, for instance, would be to retrieve several short cores at different slope sites and assess bulk density and strength property distributions

Fig. 9 Maps showing critical slope areas susceptible for future subaquatic sliding during a simulated small ($k = 1.5\%$ g, **a**) and strong ($k = 3.5\%$ g, **b**) future earthquake. Only data points, for which deterministic calculations reveal factors of safety < 1.1 are plotted. The color code indicates the corresponding thickness of the sedimentary slope cover that would be mobilized if failure occurs, and can be considered as a first-order “proxy” for the tsunamigenic potential of future landslides. Arrows in **b** indicate areas revealing a higher susceptibility for tsunamigenic landslides (Arrow labeled “a” gives localization of slope area discussed in the text)



within the uppermost 1–2 m and extrapolate these characteristics to the deeper section (e.g. Lee et al. 2000).

Also, failure criteria defined in the current limit-equilibrium infinite slope stability analysis represent simplifications that might not fully describe the generally complex dynamic processes acting on submerged slopes during seismic shaking (e.g. degradation of soft clays, accumulation of plastic strains, shear-induced excess pore-water pressure with increasing number of seismic cycles; e.g. Kreiter et al. 2010; Sultan et al. 2004; Biscontin et al. 2004). Geotechnical laboratory tests studying the dynamic behavior of the sediment, as well as campaigns monitoring in situ pore pressure conditions in critical depths over longer periods, to properly quantify excess formation pore pressure are required to improve our understanding of sediment stability and landslide initiation and will provide valuable data to refine the slope stability model.

In order to provide reliable quantitative information on earthquake intensities that affected the Lake Lucerne area during prehistoric times, as well as to reliably assess maximum values that were not exceeded, a better understanding of the relationship between the pseudo-static horizontal acceleration used and the effective peak ground acceleration (PGA) is required. Improvements might be gained from future studies comparing and calibrating critical pseudo-static accelerations calculated for failed slopes during the 1601 A.D. earthquake, with PGA values deduced from probabilistic ground motion and site effect models that simulate this historically relatively well-constrained $M_w \sim 6.2$ earthquake. Considering tsunami hazards, this study only identifies the sediment thickness at single data points that are susceptible for future subaquatic landsliding and proposes that the thickness might be used as a “proxy” for their tsunamigenic potential. However,

other parameters, such as landslide velocity and rigidity exhibit major control on tsunami generation (e.g. Trifunac and Todorovska 2002; Bardet et al. 2003) and thus need to be addressed for reliable tsunami hazard assessments. Such studies will eventually use numerical tsunami models in order to assess potential wave height and inundation scenarios.

Conclusions

Our study shows that the general concept of basin-wide mapping of critical slope stability conditions for subaquatic landslide initiation at different times in the past, during which earthquake-triggered subaquatic landslides occurred, can be considered as a promising tool for reconstructing paleo slope-stability conditions, thus providing quantitative information on intensities of past seismicity in the Lucerne area. Such quantitative information provides key input parameters for long-term earthquake models and regional probabilistic seismic assessments. Furthermore, the approach allows for a present-day basin-wide slope stability assessment and provides the means for identifying “charged” slopes susceptible for future potentially tsunami-triggered landslides.

In order to transfer this conceptual knowledge from Lake Lucerne, which is considered as a model basin, to ocean margin settings, the presented approach, however, needs to be adjusted: i.e. to take into account more complex systems with larger sediment diversity and potential failure planes occurring at different stratigraphic levels (e.g. multiple weak layers; i.e. more complex slope models with inferred slope stability back-analysis that will have more than one single-case solution). In such future studies, the analysis will ideally be performed in a probabilistic mode rather than in a simple deterministic mode and results will need to be interpreted statistically for different scenarios. Comparable slope stability conditions may evolve in fjords and high-latitude ocean margins, where glacially overconsolidated deposits are overlain by postglacial (glacio-) marine sediments accumulated during deglaciation periods and by pelagic and hemipelagic sediments deposited during interglacials (e.g. Boe et al. 2004; Locat et al. 2003). The conceptual ideas of our study thus may be vital to improve our understanding of earthquake-triggered submarine landslides and related seismic and oceanic geohazard along formerly glaciated ocean margins and closed basins worldwide. In such settings, the here-presented approach of spatially reconstructing past critical slope stability conditions through time and correlating results with the known landslide distribution may be applied if well-constrained datasets on the temporal and spatial distribution of simultaneously triggered subaquatic

landslides, as well as geological and geotechnical data from slopes that failed and slopes that remained stable during past events are available and/or can be obtained for a given study area.

Acknowledgments Bathymetric data were collected with an instrument from the Geological Survey of Norway (NGU); we thank Louise Hansen, Raymond Eilertsen and Oddbjørn Totland for their support in this bathymetry project, which was sponsored by the Swiss Confederation (swisstopo, FOEN, DDPS) and the Canton of Nidwalden. A. J. Kopf, A. Solheim and D. Giardini are acknowledged for discussion and critically commenting on earlier drafts of this manuscript. Comments by editors Peter Clift and Antonio Cattaneo, as well as two anonymous reviews improved the initial version of this manuscript. The study was supported by the Swiss National Science Foundation (grant 620-066113 and PBEZ2-118865) and the DFG-Research Centre/Cluster of Excellence “The Ocean in the Earth System”.

References

- Bardet JP, Synolakis CE, Davies HL, Imamura F, Okal EA (2003) Landslide tsunamis: recent findings and research directions. *Pure Appl Geophys* 160:1793–1809. doi:10.1007/s00024-003-2406-0
- Bay F, Wiemer S, Fäh D, Giardini D (2005) Predictive ground motion scaling in Switzerland: best estimates and uncertainties. *J Seismol* 9:223–240. doi:10.1007/s10950-005-5129-0
- Biscontin G, Pestana JM, Nadim F (2004) Seismic triggering of submarine slides in soft cohesive soil deposits. *Mar Geol* 203:341–354. doi:10.1016/S0025-3227(03)00314-1
- Boe R, Longwa O, Lepland A et al (2004) Postglacial mass movements and their causes in fjords and lakes in western Norway. *Norw J Geol* 84:35–55
- Bührer H, Ambühl H (1996) Der Vierwaldstättersee 1961–1992—Eine Dokumentation. Schriftenreihe der EAWAG, 10, 54 pp.
- Camerlenghi A, Urgeles R, Ercilla G, Brückmann W (2007) Scientific Ocean drilling behind the assessment of geo-hazards from submarine slides. *Sci Drill* 4:45–47. doi:10.2204/iodp.sd.4.14.2007
- Cysat R (1601) *Collectanea Chronica und denkwürdige Sachen pro Chronica Lucernensi et Helvetiae*. In: Schid J (ed) *Quellen und Forschungen zur Kulturgeschichte von Luzern und der Inner-schweiz*. Diebold Schilling Verlag, Luzern, pp 882–888
- De Batist M, Chapron E (2008) Lake systems: sedimentary archives of climate change and tectonics. *Palaeogeogr Palaeoclimatol Palaeoecol* 259:93–95. doi:10.1016/j.palaeo.2007.10.016
- Dugan B, Flemings PB (2000) Overpressure and fluid flow in the New Jersey continental slope: implications for slope failure and cold seeps. *Science* 289:288–291. doi:10.1126/science.289.5477.288
- Girardclos S, Schmidt OT, Sturm M, Ariztegui D, Pugin A, Anselmetti FS (2007) The 1996 AD delta collapse and large turbidite in Lake Brienz. *Mar Geol* 241:137–154. doi:10.1016/j.margeo.2007.03.011
- Gisler M, Fäh D, Kästli P (2004) Historical seismicity in Central Switzerland. *Eclogae Geol Helv* 97:221–236. doi:10.1007/s00015-004-1128-3
- Goldfinger C, Nelson CH, Johnson JE (2003) Holocene earthquake records from the Cascadia subduction zone and northern San Andreas Fault on precise dating of offshore turbidites. *Annu Rev Earth Planet Sci* 3:555–577. doi:10.1146/annurev.earth.31.100901.141246
- Gorsevski PV, Gessler PE, Boll J, Elliot WJ, Foltz RB (2006) Spatially and temporally distributed modeling of landslide

- susceptibility. *Geomorphology* 80:178–198. doi:10.1016/j.geomorph.2006.02.011
- Hampton MA, Lee HJ, Locat J (1996) Submarine landslides. *Rev Geophys* 34:33–59
- Hilbe M, Anselmetti FS, Eilertsen RS, Hansen L (2008) Spuren von Massenbewegungen auf dem Grund des Vierwaldstättersees bei Weggis: Die Ereignisse von 1601 und 1795. *Bull Angewandte Geol* 13:83–85
- Inouchi Y, Kinugasa Y, Kumon F, Nakano S, Ysumatsu S, Shiki T (1996) Turbidites as record of intense paleoearthquakes in Lake Biwa, Japan. *Sediment Geol* 104:117–125. doi:10.1016/0037-0738(95)00124-7
- Kelts K, Hsü KJ (1980) Resedimented facies of 1875 Horgen slumps in Lake Zurich as a process model of longitudinal transport of turbidity currents. *Ecologiae Geol Helv* 73:271–281
- Kreiter S, Moerz T, Strasser M, Lange M, Schunn W, Schlue BF, Otto D, Kopf A (2010) Advanced dynamic soil testing—introducing the new MARUM dynamic triaxial testing device. In: Mosher DC et al (eds) *Submarine mass movements and their consequences. Advances in Natural and Technological Hazards Series*. Springer, Berlin, pp 31–41
- Lee HJ, Edwards BD (1986) Regional method to assess offshore slope stability. *J Geotech Geoenviron Eng* 112:486–509
- Lee HJ, Locat J, Dartnell P, Israel K, Wong F (1999) Regional variability of slope stability: application to the Eel margin, California. *Mar Geol* 154:305–332. doi:10.1016/S0025-3227(98)00120-0
- Lee HJ, Locat J, Dartnell P, Minasian D, Wong F (2000) A GIS-based regional analysis of the potential for shallow-seated submarine slope failure. In: *Proceedings of 8th international symposium on landslides, Cardiff, Wales, June 26–30*, pp 917–922
- Lee HJ, Locat J, Desgagnés P, Parson JD, McAdoo BG, Orange DL, Puig P, Wong FL, Dartnell P, Boulanger E (2007) Submarine mass movements on continental margins. In: Nittrouer CA, Austin JA, Field ME, Kravitz JH, Syvitski JPM, Wiber P (eds) *Continental margin sedimentation, IAS Special Publication*, vol 37, pp 213–274
- Lemcke G (1992) Ablagerungen aus Extremereignissen als Zeitmarker der Sedimentationsgeschichte im Becken von Vitznau/Weggis (Vierwaldstättersee, Schweiz). MS thesis Thesis, Georg-August-Universität Götting, Götting, 154 pp.
- Locat J, Lee HJ (2002) Submarine landslides: advances and challenges. *Can Geotech J* 39:193–212
- Locat P, Leroueil S, Locat J, Duchesne MJ (2003) Characterisation of submarine flow-slide at Pointe-Du-Fort, Saguenay Fjord, Quebec, Canada. In: Locat J, Mienert J (eds) *Submarine mass movements and their consequences*, pp 521–529
- Mankelov JM, Murphy W (1998) Using GIS in the probabilistic assessment of earthquake triggered landslide hazards. *J Earthq Eng* 2:593–623
- Masson DG, Harbitz CB, Wynn RB, Pedersen G, Lovholt F (2006) Submarine landslides: processes triggers and hazard prediction. *Philos Trans R Soc A Math Phys Eng Sci* 364:2009–2039. doi:10.1098/rsta.2006.1810
- Miles SB, Keefer DK (2000) Evaluation of seismic slope-performance models using a regional case study. *Environ Eng Geosci* 6:25–39
- Moernaut J, De Batist M, Charlet F, Heirman K, Chapron E, Pino M, Brummer R, Urrutia R (2007) Giant earthquake in South-Central Chile revealed by Holocene mass-wasting events in Lake Puyehue. *Sed Geol* 195:239–256. doi:10.1016/j.sedgeo.2006.08.005
- Monecke K, Anselmetti FS, Becker A, Sturm M, Giardini D (2004) The record of historic earthquakes in lake sediments of Central Switzerland. *Tectonophysics* 394:21–40. doi:10.1016/j.tecto.2004.07.053
- Morgan JK, Silver E, Camerlenghi A, Dugan B, Kirby S, Shipp C, Suyehiro K (2009) Addressing geohazards through ocean drilling. *Sci Drill* 7:15–30. doi:10.2204/iodp.sd.7.01.2009
- Morgenstern NR (1967) Submarine slumping and initiation of turbidity currents. In: Richards AF (ed) *Mar. Geotechnique* UP, Urbana, IL, pp 189–220
- Murphy JR, O'Brien LJ (1977) The correlation of peak ground acceleration amplitude with seismic intensity and other physical parameters. *Bull Seismol Soc Am* 67:877–915
- Owen M, Day S, Maslin M (2007) Late Pleistocene submarine mass movements: occurrence and causes. *Quat Sci Rev* 26:958–978. doi:10.1016/j.quascirev.2006.12.011
- Schnellmann M, Anselmetti FS, Giardini D, McKenzie JA, Ward SN (2002) Prehistoric earthquake history revealed by lacustrine slump deposits. *Geology* 30:1131–1134. doi:10.1130/0091-7613(2002)030<1131:PEHRBL>2.0.CO;2
- Schnellmann M, Anselmetti FS, McKenzie JA, Giardini D (2005) Mass movement-induced fold-and-thrust belt structures in unconsolidated sediments in Lake Lucerne (Switzerland). *Sedimentology* 52:271–289. doi:10.1111/j.1365-3091.2004.00694.x
- Schnellmann M, Anselmetti FS, McKenzie JA, Giardini D (2006) 15,000 Years of mass-movement history in Lake Lucerne: implications for seismic and tsunami hazards. *Ecologiae Geol Helv* 99:409–428. doi:10.1007/s00015-006-1196-7
- Schwarz-Zanetti G, Deichmann N, Fäh D, Giardini D, Jimenez MJ, Masciadri V, Schibler R, Schnellman M (2003) The earthquake in Unterwalden on September 18, 1601: a historic-critical macroseismic evaluation. *Ecologiae Geol Helv* 96:441–450
- Seed HB (1979) Considerations in earthquake-resistant design of earth and rock-fill dams. *Géotechniques* 29:215–263
- Seed HB, Idriss IM (1971) Simplified procedure for evaluating soil liquefaction potential. *J Soil Mech Found Div Proc Am Soc Civil Eng* 97:1249–1273
- Siegenthaler C, Finger W, Kelts K, Wang S (1987) Earthquake and Seiche Deposits in Lake Lucerne, Switzerland. *Ecologiae Geol Helv* 80:241–260
- Stegmann S, Strasser M, Anselmetti FS, Kopf A (2007) Geotechnical in situ characterisation of subaquatic slopes: the role of pore pressure transients versus frictional strength in landslide initiation. *Geophys Res Lett* 34:L07607. doi:10.1029/2006GL029122
- Strasser M, Anselmetti FS, Fäh D, Giardini D, Schnellman M (2006) Magnitudes and source areas of large prehistoric northern Alpine earthquakes revealed by slope failures in lakes. *Geology* 34:1005–1008. doi:10.1130/G22784A.1
- Strasser M, Stegmann S, Bussmann F, Anselmetti FS, Rick B, Kopf A (2007) Quantifying subaqueous slope stability during seismic shaking: Lake Lucerne as model for ocean margins. *Mar Geol* 240:77–97. doi:10.1016/j.margeo.2007.02.016
- Sultan N, Cochonat P, Canals M, Cattaneo A, Dennielou B, Hafidason H, Laberg JS, Long D, Mienert J, Trincardi F (2004) Triggering mechanisms of slope instability processes and sediment failures on continental margins: a geotechnical approach. *Mar Geol* 213:291–321. doi:10.1016/j.margeo.2004.10.011
- ten Brink US, Barkan R, Andrews BD, Chaytor JD (2009a) Size distributions and failure initiation of submarine and subaerial landslides. *Earth Planet Sci Lett* 287:31–42. doi:10.1016/j.epsl.2009.07.031
- ten Brink US, Lee HJ, Geist EL, Twichell D (2009b) Assessment of tsunami hazard to the U.S. East Coast using relationships between submarine landslides and earthquakes. *Mar Geol* 264:65–73. doi:10.1016/j.margeo.2008.05.011

Trifunac MD, Todorovska MI (2002) A note on differences in tsunami source parameters for submarine slides and earthquakes. *Soil Dyn Earthq Eng* 22:143–155. doi:[10.1016/S0267-7261\(01\)00057-4](https://doi.org/10.1016/S0267-7261(01)00057-4)

Urgeles R, Locat J, Lee HJ, Martin F (2002) The Saquenay Fjord, Quebec, Canada: integrating marine geotechnical and geophysical data for spatial seismic slope stability and hazard assessment. *Mar Geol* 185:319–340. doi:[10.1016/S0025-3227\(02\)00185-8](https://doi.org/10.1016/S0025-3227(02)00185-8)